

Towards laboratory detection of topological vortices in superfluid phases of QCD

Arpan Das, Shreyansh S. Dave, Somnath De, and Ajit M. Srivastava
Institute of Physics, Bhubaneswar 751005, India

Topological defects arise in a variety of systems, e.g. vortices in superfluid helium to cosmic strings in the early universe. There is an indirect evidence of neutron superfluid vortices from glitches in pulsars. One also expects that topological defects may arise in various high baryon density phases of quantum chromodynamics (QCD), e.g. superfluid topological vortices in the color flavor locked (CFL) phase. We investigate the possibility of detecting these topological superfluid vortices in laboratory experiments, namely heavy-ion collisions. Using hydrodynamic simulations, we show that vortices can qualitatively affect the power spectrum of flow fluctuations. This can give unambiguous signal for superfluid transition resulting in vortices, allowing for check of defect formation theories in a relativistic quantum field theory system.

PACS numbers: PACS numbers: 11.27.+d, 98.80.Cq, 25.75.-q

Topological defects are typically associated with symmetry breaking phase transitions. Due to their topological nature, they display various universal properties, especially in their formation mechanism and evolution. This has led to experimental studies of defect formation in a range of low energy condensed matter systems, providing test of the theory of cosmic defect formation proposed by Kibble [1], usually known as the Kibble mechanism. The Kibble mechanism was originally proposed in the context of topological defects in grand unified theory (GUT) phase transitions in the early universe. It was pointed out by Zurek that this mechanism can be tested in superfluid helium system [2]. Indeed, a range of experimental investigations in superfluid helium, superconductors, liquid crystals etc. [3] have provided experimental checks on different aspects of the *cosmic defect formation theory*.

It is interesting that a theory originally proposed in the context of relativistic quantum field theory systems has been subjected to experimental tests in low energy, non-relativistic, condensed matter systems, often requiring only classical treatment (e.g. for liquid crystals). This has been possible due to various universal properties of these topological defects. At the same time, it is clearly desirable to experimentally test these theories also in a relativistic quantum field theory system for a more direct correspondence with the theory of cosmic strings and other cosmic defects. We address this possibility in this paper and focus on relativistic heavy-ion collision experiments which have provided remarkable insights into properties of hadronic matter in extreme conditions and its transition to the quark-gluon plasma (QGP) phase. One of the main aims of these experiments is to probe the QCD phase diagram which shows very rich features, especially in the regime of high baryon density and low temperatures. FAIR and NICA are upcoming facilities for heavy-ion collisions, dedicated to the investigation of high baryon density phases of QCD. Exotic partonic phases e.g. two flavor color superconducting (2SC) phase, crystalline color superconducting phase, color flavor locked (CFL) phase, [4] etc. are possible at very high baryon density. Even at moderately low baryon densities

nucleon superfluidity (neutron superfluidity and proton superconductivity) arises. Transitions to these phases is associated with complex symmetry breaking patterns allowing for a very rich variety of topological defects in different phases.

In the present day universe, the interior of a neutron star provides physical conditions where transition to these phases may be possible. Superfluid phases of nucleons are expected to exist inside neutron stars [5] and resulting vortices are supposed to be responsible for the phenomenon of glitches [6]. No such observational support exists yet for the high density phases of QCD (e.g. CFL phase) in any astrophysical object. In an earlier paper, some of us have proposed the detection of such phase transitions by studying density fluctuations arising from topological defect formation and its effects on pulsar timings and gravitational wave emission [7].

All of the relativistic heavy-ion collision investigations (theoretical as well as planned experiments) probing the high baryon density regime of QCD have focused primarily on signals related to the quark-hadron transition. We propose a somewhat different line of focus at these experiments. Some of these exotic high baryon density partonic phases also have superfluidity. For example, the CFL phase corresponds to the spontaneous symmetry breaking pattern, $SU(3)_{color} \times SU(3)_L \times SU(3)_R \times U(1)_B \rightarrow SU(3)_{color+L+R} \times Z_2$. Superfluidity arises from spontaneous breaking of $U(1)_B$ to Z_2 as the diquark order parameter for the CFL phase is not invariant under $U(1)_B$ baryon number transformations. This is also expected in somewhat lower density phases (where effects of heavier strange quark become important) such as the 2SC phase [4]. In heavy-ion collision experiments, if any of these phases arise, a superfluid transition will inevitably lead to production of superfluid vortices via the Kibble mechanism [1]. Universality of defect formation in the Kibble mechanism tells that defect density of order one will be produced per correlation domain [1]. (For a second order transition, the relevant correlation length can have very sensitive dependence on the rate of cooling etc. due to critical slowing down, and defect formation in such situation is described by the Kibble-Zurek mechanism[2].)

It is immediately obvious that the most dramatic effect of presence of any vortices will be on the resulting flow pattern. We carry out detailed simulations of development of flow in the presence of vortices and study qualitative changes in the flow pattern. We find three distinctive signals for the presence of vortices. These are, development of strong directed flow, a systematic variation of power spectrum for even and odd flow coefficients, and in certain situations, negative elliptic flow for non-central collisions.

We further propose that it will be worthwhile to also probe the low baryon density, low temperature regime, at these experiments, which may lead to superfluid nucleonic phase as in the interior of a neutron star [6]. Though neutron superfluid condensate is expected to exist inside several nuclei, these systems are too small to demonstrate bulk superfluid phase and its associated superfluid vortices as are expected inside a neutron star. By carrying out the heavy-ion collisions at very low energies, less than 1 GeV lab energy, utilizing appropriate nuclei (heaviest possible nuclei, presumably near the neutron dripline, which may be possible at FAIR and NICA), one may be able to create bulk nucleonic superfluid phase. Kibble mechanism will then lead to production of superfluid vortices, which will again lead to the distinctive signals we find in our hydrodynamical simulations (as expected from the universality of defect formation and evolution). This can allow experimental study of these nucleonic superfluid vortices, thereby providing valuable insight in our understanding of pulsars.

We will first focus on superfluid transitions in the high baryon density partonic phase of QCD and later comment on the possibility of low baryon density nucleonic superfluid phase transition. It is known that various high baryon density partonic phases (QGP, 2SC, CFL etc.) do not differ much in energy density and pressure [4]. Most important difference is in the symmetry properties of the condensate. We carry out hydrodynamical simulations of the evolution of a partonic system in the presence of vortices using a two-fluid picture of superfluid. We also consider a range of values for the fraction of superfluid to normal fluid and study its effect on the signals. Normal fluid is evolved with standard initial conditions, as in our earlier simulations [8], with Woods-Saxon profile of energy density with and without additional density fluctuations (to model realistic situation where initial state density fluctuations are always present, though it does not appear to have crucial effects on our results). As discussed above, we evolve the superfluid component with the same equation of state as the normal fluid, but with a velocity pattern corresponding to presence of vortices in the superfluid part. The equation of state is taken simply to be an ideal gas of quarks and gluons at temperature T and quark chemical potential μ_q with the energy density ϵ given as (for two light flavors) [9],

$$\epsilon = \frac{6}{\pi^2} \left(\frac{7\pi^4}{60} T^4 + \frac{\pi^2}{2} T^2 \mu_q^2 + \frac{1}{4} \mu_q^4 \right) + \frac{8\pi^2}{15} T^4 \quad (1)$$

with pressure $P = \epsilon/3$. Note, as our interest is only in discussing the hydrodynamics in the partonic phase (and not in the quark-hadron transition), we do not include the bag constant. The energy-momentum tensor is taken to have the perfect fluid form,

$$T^{\mu\nu} = (\epsilon + P) u^\mu u^\nu - P g^{\mu\nu} \quad (2)$$

where u^μ is the fluid four-velocity. The hydrodynamical evolution is carried out using the equations, $\partial_\mu T^{\mu\nu} = 0$. Note that we do not need to use conservation equation for the baryon current as our interest is only in flow pattern requiring knowledge of ϵ and P and the ideal gas equation of state relating P and ϵ does not involve μ_q . The simulation is carried out using a 3+1 dimensional code with leapfrog algorithm of 2nd order accuracy. For various simulation details we refer to the earlier work [8]. The initial energy density profile for both fluid components (normal fluid as well as superfluid) is taken as a Woods-Saxon background of radius 3.0 fm with skin width of 0.3 fm. There is much uncertainty about the value of μ_q and T at which one expects the phase transition to these novel phases of QCD [4]. We take the initial central energy density ϵ_0 with temperature $T_0 = 25$ MeV and $\mu_q = 500$ MeV. Initial random fluctuations are incorporated in terms of 10 Gaussian of half-width 0.8 fm, with central amplitude taken to be $0.4\epsilon_0$.

Normal fluid is taken to have zero velocity initially, while the superfluid part includes the fluid rotation around the vortices. The magnitude of the fluid rotational velocity at distance r from the vortex center is taken as

$$\begin{aligned} v(r) &= v_0 \frac{r}{\xi} \quad \text{for } r \leq \xi \\ &= v_0 \frac{\xi}{r} \quad \text{for } r > \xi \end{aligned} \quad (3)$$

Here ξ is the coherence length. For CFL vortex, estimates in ref.[5] give $v_0 = 1/(2\mu_q \xi)$ and the coherence length is given by

$$\xi \simeq 0.26 \left(\frac{100 \text{ MeV}}{T_c} \right) \left(1 - \frac{T}{T_c} \right)^{-1/2} \text{ fm.} \quad (4)$$

We take value of superfluid transition temperature $T_c = 50$ MeV [5]. For the initial central temperature $T_0 = 25$ MeV, resulting values of $\xi = 0.7$ fm and $v_0 = 0.3$. (Note, even though we use 2 flavors, we use the estimates of the vortex profile for the CFL phase for order of magnitude estimates.) We mention that we do not simulate coupled dynamics of normal and superfluid components. Instead, we evolve the two components using separate conservation equations for the two energy

momentum tensors. This allows us to simulate a delayed superfluid transition. This models the situation when initial partonic system has too high a temperature to be in the superfluid phase, though it is still in the QGP phase, and subsequent expansion and cooling leads to crossing the phase boundary to the superfluid phase. Also, for the case of nucleon superfluidity (to be discussed below), initial high temperatures will lead to normal nucleonic phase, and only at late stages of expansion superfluid phase can arise. In a coupled fluid dynamics, this cannot be achieved as one always has a normal fluid as well as a superfluid component.

For observational signatures, we focus on the power spectrum of flow fluctuations. In a series of papers some of us have demonstrated that just like the power spectrum of CMBR, in heavy-ion collisions also the power spectrum of flow fluctuations has valuable information about the initial state fluctuations of the plasma [10]. We will calculate the power spectrum of flow fluctuations and study the information contained in the power spectrum about the initial vortex induced velocity fields. We focus on the central rapidity region (focusing on a thin slab of width 2 fm in z direction at $z = 0$) and study the angular anisotropy of the fractional fluctuation in the fluid momentum, $\delta p(\phi)/p_{av}$, where ϕ is the azimuthal angle and p_{av} is the angular average of the fluid momentum. This fluid momentum anisotropy is eventually observed as momentum anisotropy of the hadrons which are finally detected. The power spectrum of flow fluctuations is obtained by calculating the root mean square values v_n^{rms} of the n th Fourier coefficient v_n of the momentum anisotropy $\delta p(\phi)/p_{av}$.

We use standard Kibble mechanism to estimate the probability of vortex formation. In the CFL phase, superfluidity corresponds to spontaneous breaking of U(1) symmetry (just like the case for superfluid ^4He). In two space dimensions, this leads to probability 1/4 for the formation of a vortex or antivortex per correlation domain [1]. For the azimuthal momentum anisotropy in the central rapidity region, the relevant velocity field is essentially two-dimensional. With the correlation length of order 1 fm, and the plasma region of a radius of 3 fm, we expect number of superfluid vortices to be about 2. For definiteness, we will consider cases of 1 vortex, and a vortex-vortex pair and a vortex-antivortex pair. The locations of these are taken to be randomly distributed in the plasma region. To have clear signals, we have taken definite orientations for the vortices. We consider vortices either pointing along z axis (with random locations) or pointing along x axis (passing through the origin).

We now present results of the simulations. Fig.1 shows the velocity fields of the central rapidity region in the transverse plane at $\tau - \tau_0 = 0.84$ fm/c for the case without any vortex as well as the case when a vortex-antivortex pair contributes to the net velocity (net velocity is taken with suitable weights for the normal fluid and superfluid parts). Both cases correspond to central collisions leading to roughly isotropic region, along with few

initial state density fluctuations. Clearly the flow field undergoes dramatic changes in the presence of vortices resulting in various signals we find. (The plots in Fig.1 as well as in rest of the paper were obtained by taking the superfluid component to be the dominant one (90%) over the normal fluid part (10%). We find that various signals decrease proportionally as superfluid percentage is decreased, as we will show in Fig.2.)

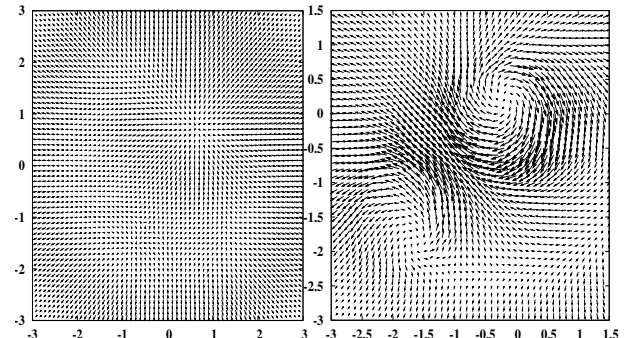


FIG. 1: Left figure shows the velocity fields for the case without any vortex and right figure shows the velocity field when a vortex-antivortex pair contributes to the net velocity.

Fig.2 shows the effect of vortices on the flow power spectrum for a central collision at $\tau - \tau_0 = 1.68$ fm. We mention that due to complexity of flow pattern, fluid evolution becomes unstable for large times, hence we show the results at relatively shorter times. However, these qualitative signals will be expected to survive even for longer times. As such these will apply to situations of early freezeout, e.g. for smaller nuclei, or for peripheral collisions. Solid plot shows the power spectrum in the absence of any vortex. The dotted, dash-dotted, and dot-dotted plots show the cases for a vortex, a vortex-vortex pair, and a vortex-antivortex pair respectively. In all cases, vortices are taken along the z axis with random positions. Noteworthy is the presence of non-zero value of v_1^{rms} (directed flow) in the presence of vortices. Largest value of directed flow occurs for the case with vortex-antivortex pair as one can anticipate from the flow pattern in Fig.1. Such large values of directed flow are not expected in any other situation (small directed flow can result from initial state density fluctuations). We have also studied the effect of varying the proportion of superfluid. As expected, the effects associated with superfluid vortices decrease roughly proportionally as the superfluid proportion is decreased. For example, the directed flow (v_1^{rms}) for the case of a single vortex increases with increase in the superfluid proportion as shown in the inset in Fig.2.

Fig.3 shows the time evolution of the power spectrum for the case with a vortex-vortex pair. Note difference in the power for even and odd Fourier coefficients at earlier times. (Such a qualitatively different pattern in heavy-ion collisions has only been predicted in the presence of magnetic field, as reported in ref. [11]). This result also has interesting implications for the CMBR power spec-

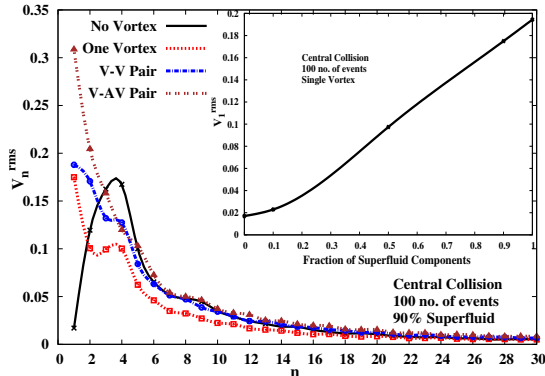


FIG. 2: Power spectrum at $\tau - \tau_0 = 1.68$ fm. Solid plot shows the power spectrum in the absence of any vortex. The dotted, dash-dotted, and dot-dotted plots show the cases for a vortex, a vortex-vortex pair, and a vortex-antivortex pair respectively showing non-zero v_1^{rms} (directed flow) for central collision with 90% superfluid component. The inset shows the dependence of directed flow on the proportion of superfluid component for the case of single vortex.

trum. It is known that low l modes of CMBR power spectrum also show difference in even-odd modes [12]. It is possible that this feature may be indicative of the presence of a magnetic field, or presence of some vorticity during the very early stages of the inflation. We hope to present investigation of this very intriguing possibility in a future work.

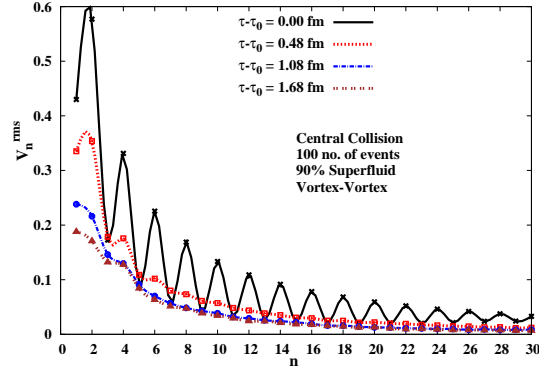


FIG. 3: Time evolution of the power spectrum for the case with a vortex-vortex pair showing the difference in the power for even and odd Fourier coefficients for early times.

Fig.4 presents the case of vortex lying along the x axis. Here we consider an ellipsoidal shape for the plasma region as appropriate for a non-central collision with initial spatial eccentricity = 0.6, and plot the time evolution of the momentum eccentricity ϵ_p which is directly related to v_2 , and is a more convenient quantity to use for hydrodynamics simulation [13]. It is defined in terms of components of energy momentum tensor (Eqn.(2)) as $\epsilon_p = (T^{xx} - T^{yy})/(T^{xx} + T^{yy})$. Comparison with the case without any vortex shows negative values of ϵ_p for the case with the vortex at early times. ϵ_p eventually

becomes positive. (Here we also show a case with large $T_c = 80$ MeV with corresponding $\xi = 0.4$ fm and $v_0 = 0.5$, leading to stronger negative elliptic flow). This negative elliptic flow may be observed if the freezeout occurs at early times (in smaller systems, or in peripheral collisions) and may also leave imprints on other observables such as on v_2 for photons [14].

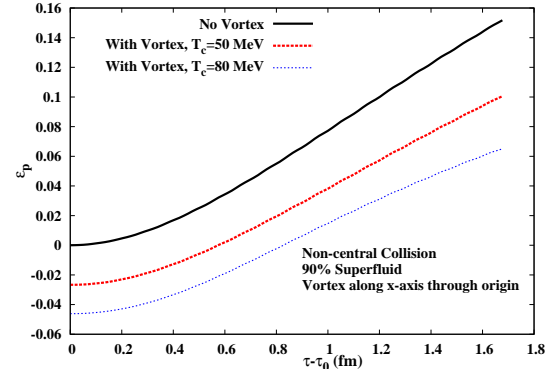


FIG. 4: Plot of time evolution of the momentum eccentricity ϵ_p for the case without any vortex (solid curve) and the case with a vortex lying along the x axis for a non-central collision (dashed curve for $T_c = 50$ MeV and dotted curve for $T_c = 80$ MeV) showing negative values of ϵ_p at early times.

We have carried out all the simulations with a delay of up to 1 fm in the onset of superfluid transition (following our modeling of the two fluid picture as explained above). The results remain essentially unchanged with various plots showing changes of order only few percent.

We now comment on the possibility of detecting nucleonic superfluidity in heavy-ion collisions. Calculations for neutron stars show that nucleonic superfluidity is expected in range of densities from $10^{-3}\rho_0$ (for 1S_0 pairing of neutrons) to few times ρ_0 (for $^3P_2 - ^3F_2$ pairing). The critical temperature can range from 0.2 MeV to 5 MeV (depending on the nuclear potential used [15]). Temperatures and densities of this order are easily reached in heavy-ion collisions at relatively low energies. For example, at the FOPI-facility at GSI Darmstadt, temperatures of about 17 MeV (with $\rho \sim 0.4\rho_0$) were reached in Au-Au collisions at 150 MeV/nucleon lab energy [16]. Temperatures of order 4-5 MeV were reported in Au-Au collisions at $E/A = 50$ MeV, at heavy-ion synchrotron SIS [17]. Thus temperatures/densities appropriate for the transition to the nucleonic superfluid phase can easily be reached in heavy-ion collisions. FAIR and NICA are ideal facilities for probing even this low energy regime with detectors suitable for measurements with which flow power spectrum analysis can be performed. Detection of signals as discussed in this paper can provide a clean detection of nucleonic superfluid vortices. It is worth emphasizing the importance of focused experiments for creating a nucleonic system of several fm size which can accommodate nucleonic superfluid vortices. Direct experimental evidence of these vortices and controlled studies of their

properties can provide a firm basis for our understanding of neutron stars. This is all the more important in view of the fact that gravitational waves from neutron stars and their collisions will be thoroughly probed by LIGO and upcoming gravitational wave detectors.

We conclude by pointing out that the signals we have discussed show qualitatively new features in flow anisotropies signaling the presence of vortices and the underlying superfluid phase in the evolving plasma region. These qualitative features are expected to be almost model independent, solely arising from the vortex velocity fields. Similar signals are expected from nucleonic superfluid vortices which can arise in low energy

heavy-ion collisions providing direct experimental access to the physics of pulsars. Detection of these vortices will allow probing Kibble mechanism for these relativistic quantum field theory systems, providing a more direct correspondence with the theory of cosmic defects. For second order transitions, one will also be able to use the Kibble-Zurek mechanism to probe the effects of critical slowing down and gain knowledge of various critical exponents for the specific transition.

We are very grateful to Rajeev Bhalerao, Partha Bagchi, Srikumar Sengupta, Biswanath Layek, and Pranati Rath for useful discussions.

- [1] T.W.B. Kibble, J. Phys. **A 9**, 1387 (1976); Phys. Rep. **67**, 183 (1980)
- [2] W.H. Zurek, Nature **317**, 505 (1985); Phys. Rep. **276**, 177 (1996).
- [3] See, for example, special section on condensed matter analogues of cosmology, J. Phys. **G 25** (2013).
- [4] M.G. Alford, A. Schmitt, K. Rajagopal, and T. Schafer, Rev. Mod. Phys. **80**, 1455 (2008).
- [5] K. Iida and G. Baym, Phys. Rev. **D 66**, 014015 (2002).
- [6] J.M. Lattimer and M. Prakash, Astrophys. J. **550**, 426 (2001).
- [7] P. Bagchi, A. Das, B. Layek, and A.M. Srivastava, Phys. Lett. **B 747**, 120 (2015); arXiv: 1412.4279.
- [8] Saumia P.S. and A.M. Srivastava, arXiv: 1512.02136.
- [9] J. Cleymans, R.V. Gavai, and E. Suhonen, Phys. Rep. **130**, 217 (1986).
- [10] A. P. Mishra, R. K. Mohapatra, P. S. Saumia, and A. M. Srivastava, Phys. Rev. **C 77**, 064902 (2008); Phys. Rev. **C 81**, 034903 (2010).
- [11] A.M. Srivastava, Talk presented in the conference *QCD Chirality Workshop 2015* at Physics Dept. UCLA, Jan. 2015.
- [12] P. K. Aluri and P. Jain, Mon. Not. Roy. Astron. Soc. **419**, 3378 (2012).
- [13] P.F. Kolb, J. Sollfrank, and U. Heinz, Phys. Rev. **C 62**, 054909 (2000).
- [14] R. Chatterjee and D. K. Srivastava, Nucl.Phys. **A 830**, 503C (2009).
- [15] L. Amundsen and E.Ostgaard, Nucl. Phys. **A 442**, 163 (1985), *ibid*, **A 437**, 487 (1985).
- [16] W. Reisdorf, et al., Nucl. Phys. **A 612**, 493 (1997), nucl-ex/9610009
- [17] V. Serfling et al., Phys. Rev. Lett. **80**, 3928 (1998), nucl-ex/9801006